JOC The Journal of Organic Chemistry

Article

pubs.acs.org/joc

Alkoxyamine Re-Formation Reaction. Effects of the Nitroxide Fragment: A Multiparameter Analysis.

Elena G. Bagryanskaya,[†,⊥] Sylvain R. A. Marque,*[,‡,§] and Yuri P. Tsentalovich[†]

[†]International Tomography Center SB RAS, Institutskaya 3A, 630090 Novosibirsk, Russia Federation

[⊥]V. V. Vorozhsov Novosibirsk Institute of Organic Chemistry SB RAS, Pr. Lavrentjeva 16, Novosibirsk, 630090, Russian Federation

[‡]Aix-Marseille Université, ICR-UMR7273, case 521, Avenue Escadrille Normandie-Niemen, 13397 Marseille cedex 20, France

[§]CNRS, ICR-UMR7273, case 521, Avenue Escadrille Normandie-Niemen, 13397 Marseille cedex 20, France

ABSTRACT: A few years ago, Studer and co-workers (*Macromolecules* **2006**, *39*, 1347−1352) reported the dramatic effect of the reaction of re-formation of alkoxyamines on the fate of the nitroxide-mediated polymerization (NMP) of styrene. This prompted us to investigate more carefully the effects of the nitroxide structure on the re-formation rate constant k_c. Ten new values of k_c were obtained for the reaction of imidozalidine nitroxide and the phenethyl radical. These values were combined with the 21 values of k_c reported in the literature for a multiparameter analysis ($\log(k_c/M^{-1}\ s^{-1}) = (10.22 \pm 0.10) + (0.46 \pm 0.02)E_s + (0.41 \pm 0.17)\sigma_I$) using the electrical Hammett constant σ_I to describe both the stabilization and polar effects as well as the modified Taft steric constant E_s of the nitroxide. The same analysis was performed for the k_c values of the cross-coupling reaction of nitroxides with *tert*-butoxylcarbonyl-2-prop-2-yl radical ($\log(k_c/M^{-1}\ s^{-1}) = (11.10 \pm 0.25) + (0.57 \pm 0.05)E_s + (1.42 \pm 0.18)\sigma_I$) and *tert*-butoxycarbonylethyl radical ($\log(k_c/M^{-1}\ s^{-1}) = (10.23 \pm 0.16) + (0.35 \pm 0.03)E_s + (0.93 \pm 0.25)\sigma_I$). These correlations were applied for the analysis of the NMP of styrene controlled by $6\pi^\bullet$, $6\theta^\bullet$, and $6\rho^\bullet$ using a Fischer phase diagram.

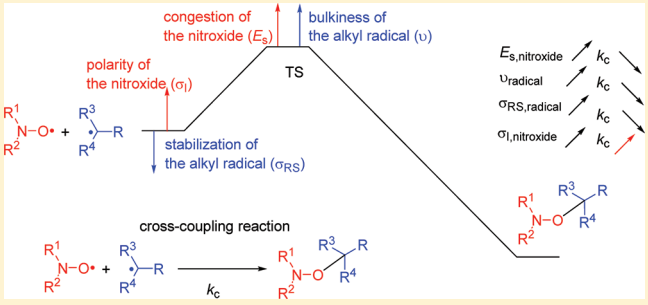

INTRODUCTION

Since the pioneer work of Rizzardo and co-workers,[1] nitroxide-mediated polymerization (NMP) has commonly been used for the preparation of highly valuable polymers and nanomaterials.[2−4] Although tremendous efforts have been devoted to the investigation of the factors ruling the kinetics[5−12] of NMP and to the preparation and investigation of new initiators/controllers,[12−16] there remain some challenges (such as homo- and block copolymerization of MMA, polymerization of vinylacetate, etc.) requiring investigation.[3,4,7,12] In a recent review,[12] it was shown that each stage—initiation, propagation, and termination (Scheme 1)—is important for the fate of the polymerization. It was pointed out that the Fischer phase diagram is a powerful tool to predict the behavior of the polymerization that depends on the nitroxide controller and, hence, to guide the design of new nitroxides/alkoxyamines.[12] Indeed, this approach affords valuable analyses as long as both the rate constant $k_{d,ds}$ of the C−ON bond homolysis and $k_{c,ds}$ of the re-formation of the dormant species ds (macro alkoxyamine, reactions 5 and 4) as well as those of the initiating alkoxyamine (k_d and k_c; reactions 1 and 2, respectively) are accurately estimated. Other rate constants (initiation k_{add}, propagation k_p, and self-termination $k_{t,ds}$; reactions 3, 6, and 7, respectively) do not depend on the alkoxyamine properties, except for the side reactions involving H-transfer reactions (k_{dD} and k_{cD}, reactions 8 and 9, respectively).

Scheme 1. NMP Scheme

Initiation

$R^1R^2NOR \longrightarrow R^1R^2NO^\bullet + R^\bullet$ (1) k_d

$R^1R^2NO^\bullet + R^\bullet \longrightarrow R^1R^2NOR$ (2) k_c

$R^\bullet + M \longrightarrow R{-}M_1^\bullet$ (3) k_{add}

Propagation

$R^1R^2NO^\bullet + RM_n^\bullet \longrightarrow R^1R^2NOM_nR$ (4) $k_{c,ds}$

$R^1R^2NOM_nR \longrightarrow R^1R^2NO^\bullet + RM_n^\bullet$ (5) $k_{d,ds}$

$RM_n^\bullet + nM \longrightarrow RM_n^\bullet$ (6) k_p

Termination

Self-termination

$R^\bullet + RM_n^\bullet \longrightarrow$ dead products (7) $k_{t,ds}$

Cross side-reactions

$R^1R^2NOR \longrightarrow R^1R^2NOH$ + alkene (8) k_{dD}

$R^1R^2NO^\bullet + R^\bullet \longrightarrow R^1R^2NOH$ + alkene (9) k_{cD}

In the past few years, the effects which have an influence on the C−ON homolysis rate constants have been carefully investigated using both experimental[13] and theoretical[17,18] approaches, and several relationships are now available to predict the value of k_d.[19−21] On the other hand, multiparameter analyses of the effects of the bulkiness and the polarity of the

Received: March 6, 2012
Published: April 23, 2012

dx.doi.org/10.1021/jo300459z | *J. Org. Chem.* 2012, 77, 4996−5005

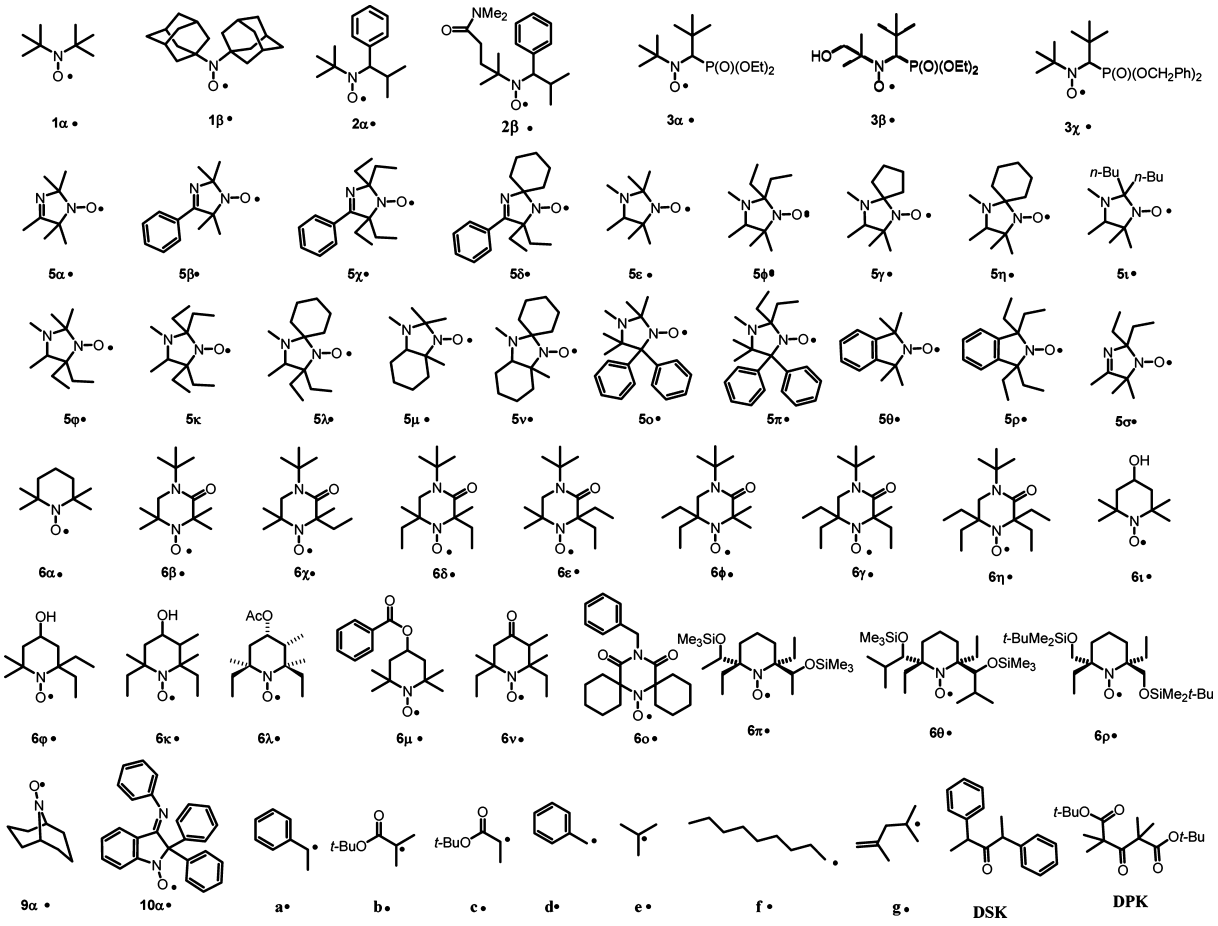

Figure 1. Molecules investigated.

groups flanking the nitroxyl moiety as well as the stabilization of the nitroxide on k_c values are scarce.[17,22−24] A first attempt to find the correlations between a steric parameter Ω, the spin density, and the k_c values reported for some nitroxides by Ingold and co-workers[25,26] was made by Iwao et al.[22] Recently, Coote and co-workers[17] reinvestigated such types of correlations for a small series of nitroxides, applying high-level calculations, except that the results were matched to only a few experimental values. It was shown that k_c decayed with increasing congestion around the nitroxyl moiety, confirming the observations reported by Fischer and co-workers[27] for the series of nitroxides ***6β•−6η•***; i.e., k_c decreased monotonically with the size of the substituents attached to the nitroxyl moiety. Recently, it was shown that the polar effect of the substituents attached to the nitroxyl moiety may also play a substantial role, depending on the type of alkyl radical.[23] In this article, we present the k_c values for the cross-coupling of phenethyl radical **a•** (Figure 1) with a series of 10 new nitroxides (Table 1) and the subsequent multiparameter analysis of the effects controlling this reaction for a larger series[25−31] of nitroxides (Figure 1). For comparison, this multiparameter approach was also applied to the k_c values for the cross-coupling of *tert*-butoxycarbonyl-2-prop-2-yl radical[23,29,32,33] **b•** and of *tert*-butoxycarbonylethyl radical[23,32−34] **c•** and various nitroxides (Figure 1).

RESULTS

Measurements of k_c. The photolysis of distyryl ketone (DSK) proceeded via the Norrish type 1 cleavage: from the triplet excited ketone fragments to **a•** and acyl radicals. The latter underwent rapid decarbonylation, affording the same stabilized styryl radical **a•** and carbon monoxide (reactions 10−12, Scheme 2). The alkyl radicals decayed in self-termination reactions, yielding dimer in the dimerization reaction, and alkane R-H and alkene R(-H) in the disproportionation reaction (eq 13). In the presence of nitroxide $R^1R^2NO•$, alkoxyamine R^1R^2NOR was formed (eq 14). The same holds for DPK (**b•** for **R•**).[23]

Scheme 2. Generation of a• from DSK (or b• from DPK) and Subsequent Reactions ([a])

$$\mathbf{a}_2C{=}O \longrightarrow [\mathbf{a}_2C{=}O]^* \quad (10)$$

$$[\mathbf{a}_2C{=}O]^* \longrightarrow \mathbf{a}\bullet + \mathbf{a}C(\bullet){=}O \quad (11)$$

$$\mathbf{a}C(\bullet){=}O \longrightarrow \mathbf{a}\bullet + CO \quad (12)$$

$$\mathbf{a}\bullet + \mathbf{a}\bullet \longrightarrow \mathbf{a}_2 + \mathbf{a}\text{-H} + \mathbf{a}(\text{-H}) \quad (13)$$

$$\mathbf{a}\bullet + R^1R^2NO\bullet \longrightarrow R^1R^2NO\mathbf{a} \quad (14)$$

[a] **a•** is given as an example.

The decay of radical **a•** (or **b•**) in the photolysis of DSK (or DPK) in the presence of different nitroxides was measured by LFP at a wavelength of 323 nm. It was found that the decay rate constant k_{obs} was directly proportional to the concentration of nitroxide, as given in eq 15, and the k_c values were determined from the slope of the plot k_{obs} vs $[R^1R^2NO•]$ (Figure 2). All k_c values are given in Table 1.

dx.doi.org/10.1021/jo300459z | J. Org. Chem. 2012, 77, 4996−5005

$$k_{obs} = k_0 + k_c[R^1R^2NO^\bullet] \quad (15)$$

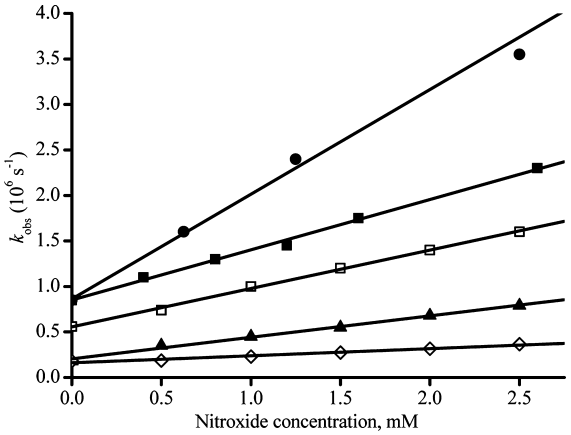

Figure 2. Dependence of k_{obs} on the concentration of nitroxides **5π•** (■), **5γ•** (●), **5κ•** (▲), **5φ•** (◇), and **5η•** (□) at 23 °C in benzene as solvent for their coupling with **a•**.

Table 1. Values of k_c[a] Measured in Benzene at 23 °C with a•, unless Otherwise Mentioned

nitroxides	k_c (10^7 L mol^{-1} s^{-1})	nitroxides	k_c (10^7 L mol^{-1} s^{-1})
5β•	24.0[b]	**5κ•**	2.2
5ε•	11.8	**5λ•**	1.3
5φ•	8.7	**5ν•**	8.1
5γ•	11.5	**5ο•**	7.0
5η•	4.3	**5π•**	5.5
5φ•	6.4	**5σ•**	17.0[b]

[a]Errors of 10%. [b]Measured for the radical **b•**.

Geometry of the Nitroxide. The electronic structure of nitroxides has been well documented for decades.[35] It can be represented by two canonical forms: the zwitterionic form **A** and the neutral form **B** (Scheme 3). The three-electron bond accounts for the strong stabilization of the nitroxide moiety, and the presence of the zwitterionic form **A** makes the stabilization of the nitroxide sensitive to the polarity—mainly the electron-withdrawing capacity—of the substituents R^1 and R^2: i.e., greater the electron-withdrawing capacities of R^1 and R^2, the less stabilized the nitroxide.

Scheme 3. Electronic Structure of Nitroxide

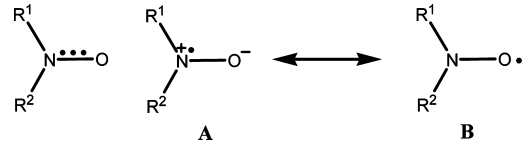

Along with the polar effect, the congestion around the nitroxyl moiety also plays an important role in the cross-coupling reaction, and its influence is expected to depend on the conformation of the alkyl groups R^1 and R^2 attached to the NO• moiety. Hence, the nitroxides investigated in this article were split into 10 families, as displayed in Figure 3.[36] For the sake of simplicity, it was assumed that there was no difference in bulkiness between the (pseudo)axial and (pseudo)equatorial positions (vide infra) for the cyclic nitroxides[37] and no steric influence for the substituents lying in the nodal plane and antiperiplanar to the N−O• moiety as well as for those far from the nitroxyl moiety.

The families displayed in Figure 3 were selected on the grounds of the X-ray analysis of several models combined with the EPR hyperfine coupling constants in solution. It has to be mentioned that these conformations, especially the position of the alkyl groups flanking the N−O• moiety, are in good agreement with the conformations revealed by X-ray analysis reported for alkoxyamines, except for the flattening of the N−O• moiety and slightly different angles. For diadamantyl nitroxide **1β•** (Figure 4a) belonging to the **1•** family,[38] X-ray data show one methyl-like group in the conformation syn to the N−O• bond, whereas the other methyl-like is in the anti conformation. This conformation is also expected for the *tert*-butyl groups of **1α•**. For the **2•** family, the X-ray structure[39] of **2β•** shows the H_β atom lying in the nodal plane and in the antiperiplanar position to the N−O• bond and shows that one of the methyl groups of the *t*-Bu moiety is in the position syn to the N−O• bond (Figures 4b and 3). The small EPR hyperfine coupling $a_{H,\beta}$ for the H atom attached at position β of the nitroxyl moiety ($a_{H,\beta}$ = 0.24 mT) in **2α•**[40] supports in solution the conformation revealed by X-ray data. The X-ray structures of **3β•**[41,42] and **3χ•** (homologue of **3α•**)[43] belonging to the **3•** family show the H_β atom in the nodal plane and in an antiperiplanar position to the N−O• bond (Figure 4c,d, respectively). They also show a bisectional position of the nitroxyl moiety between the substituents attached to the carbon at the α-position of the nitroxyl moiety (Figures 3 and 4c,d).[44] The small EPR hyperfine coupling $a_{H,\beta}$ for the H atom attached at position β of the nitroxyl moiety ($a_{H,\beta} \approx 0$ mT)[41] of **3α•** supports in solution the conformation revealed by X-ray data.

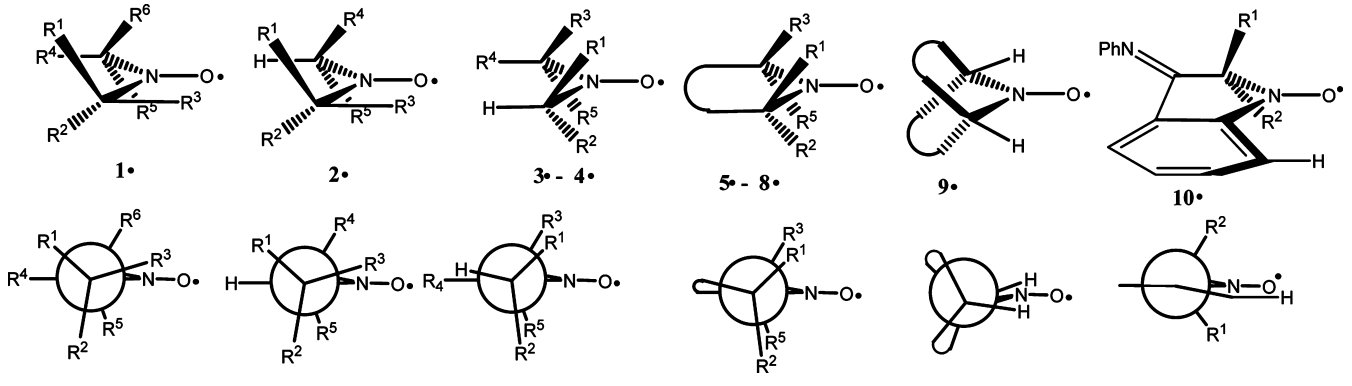

Figure 3. Newman projections around the nitroxide moiety for the nitroxide families **1•**−**10•**.

dx.doi.org/10.1021/jo300459z | J. Org. Chem. 2012, 77, 4996−5005

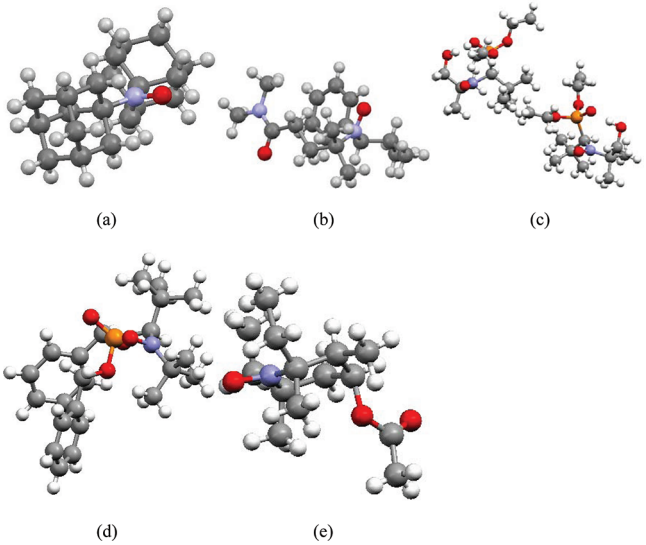

Figure 4. X-ray structures of (a) **1β•**,[38] (b) **2β•**,[39] (c) *R* and *S* enantiomers of **3β•**,[41] (d) **3χ•**,[43] and (e) **6λ•**.[21]

This peculiar conformation of the alkyl groups attached to the nitroxyl moiety for families **2•** and **3•** causes the shielding of both the nitroxyl moiety and the H atom in the β position, leading to the exceptionally long lifetimes of the nitroxides carrying an H atom in the β position.

For the **6•** family, the X-ray structure[21] of **6λ•** (Figure 4e) shows that the methyl and ethyl groups on carbons 2 and 6 are in the axial and equatorial positions, respectively. It was assumed that the same conformations at carbons 2 and 6 exist for all six-membered-ring nitroxides displayed in Figure 1.[37] For the sake of simplicity, similar conformations were assumed for the nitroxides belonging to the **5•** family. Nitroxide **9α•**,[45] belonging to the **9•** family, exhibited a conformation different from that of the other families covered in this article. The two H atoms in the β positions lay in the nodal plane of the nitroxide moiety but in a syn relationship to the N−O• bond, and therefore they were very accessible for abstraction by another radical (Figure 3). The persistence of this radical is due to Bredt's rule, which forbids the formation of a double bond by H abstraction on the bridgehead of a bicyclic compound.[45] Consequently, the presence of the two H atoms flanking the nitroxyl moiety decreases dramatically the congestion around the nitroxyl moiety and, at the same time, does not significantly alter the persistence of the nitroxide.[45] For nitroxide **10α•** (**10•** family), the indoline moiety involves a syn-1,3 interaction (1,3-A strain) between the N−O• bond and the ortho C−H bond in the aromatic ring. The conjugation of the odd electron with the aromatic ring and the phenylimino function forces the fused five-membered ring to adopt an almost planar conformation, leading the phenyl groups to exhibit a bisectional conformation with the N−O• moiety.

The Steric Effect. Monoparameter linear regressions were performed and provided good statistical outputs for the steric effect E_s (R^2 = 0.92 for **a•**, R^2 = 0.88 for **b•**, and R^2 = 0.84 for **c•**), whereas only scattered plots were observed (not shown) for the stabilization/polar effect σ_I. Values of σ_I and E_s were determined as described in the next section.

Some years ago, Fischer and co-workers[27] investigated the steric effect for the re-formation reaction of **6β•−6η•** with the alkyl radical **a•** and showed a linear decrease in log k_c with an increase in the bulkiness parameter E_s. Such a relationship is now being investigated for a larger series of nitroxides with **a•** as well as with **b•** and **c•** (parts a−c of Figure 5, respectively). The positive slopes δ' (eqs 16−18) of log k_c vs E_s for **a•−c•** point to a retarding effect due to the congestion around the nitroxide moieties, highlighted by $\delta'(\mathbf{b}^\bullet) > \delta(\mathbf{c}^\bullet)$; e.g., $\upsilon(\mathbf{b}^\bullet)$ = 1.42 and $\upsilon(\mathbf{c}^\bullet)$ = 1.01 for the tertiary alkyl radical **b•** and the secondary alkyl radical **c•**, respectively, as expected. These good correlations show that the congestion around the nitroxide moiety is the major effect controlling the cross-coupling reaction. However, some scattering, likely due to the polar/stabilization effect, led us to consider a biparameter relationship involving the polar/stabilization effect of the nitroxyl moiety.

$$\log(k_c/\mathrm{M}^{-1}\,\mathrm{s}^{-1}) = 10.18(\pm0.11) + [0.44(\pm0.02)]E_s$$
$$R^2 = 0.94 s = 0.13 N = 28 \quad (16)$$

$$\log(k_c/\mathrm{M}^{-1}\,\mathrm{s}^{-1}) = 11.04(\pm0.30) + [0.51(\pm0.05)]E_s$$
$$R^2 = 0.88 s = 0.22 N = 14 \quad (17)$$

$$\log(k_c/\mathrm{M}^{-1}\,\mathrm{s}^{-1}) = 10.36(\pm0.24) + [0.33(\pm0.05)]E_s$$
$$R^2 = 0.84 s = 0.19 N = 12 \quad (18)$$

Multiparameter Analysis. As mentioned above, the multiparameter approach for the C−ON bond homolysis was

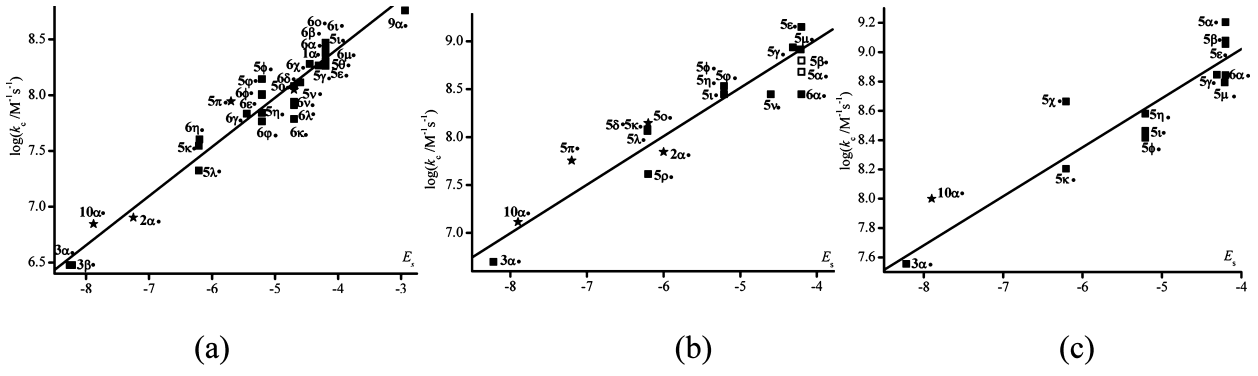

Figure 5. lg k_c at room temperature for the cross-coupling of alkyl radicals (a) **a•** in *tert*-butylbenzene, (b) **b•** in benzene, and (c) **c•** in benzene with various nitroxides (structures shown in Figure 1) vs E_s (eqs 16−18, respectively). Empty symbols denote outliers, and the asterisks denote nitroxides carrying an aromatic group attached to one carbon at the α position observed when biparameter correlations were performed.

dx.doi.org/10.1021/jo300459z | J. Org. Chem. 2012, 77, 4996−5005

shown to be very useful for analyzing and discussing the different effects influencing the value of k_d.[13,19−21,27,40,46−48] Since the C−ON bond homolysis and the re-formation reaction, which is the back reaction of the homolysis, go through the same transition state (TS),[8,12,16] it was assumed that the effects observed for the homolysis held for the re-formation reaction as well. Therefore, the k_c values for alkyl radicals **a**$^\bullet$−**c**$^\bullet$ were assumed to be correlated with the stabilization/polar (σ_I) and steric (E_s) effects, according to eq 19.[24]

$$\log(k_c/\mathrm{M}^{-1}\,\mathrm{s}^{-1}) = \log k_{c,0} + \rho'_I\sigma_I + \delta' E_s \qquad (19)$$

As pointed out above, the presence of electron-withdrawing groups (EWGs) favored form **B** over form **A** (Scheme 3),[35] increasing the density of the odd electron at the oxygen atom of the nitroxyl moiety (stabilization/polar effect). Hence, the increase in k_c is expected with the increasing polarity of the nitroxide, i.e., positive ρ'_I value. The electron-withdrawing ability of each nitroxide was given by the $\sigma_{I,n}$ values[19] determined by eq 20 (Figure 6), as reported for k_d. Individual $\sigma_I(R_i)$ values were taken from the literature and stored in Table 2.[49,50]

$$\sigma_{I,n} = \sum_{i=1}^{6} \sigma_I(R_i) \qquad (20)$$

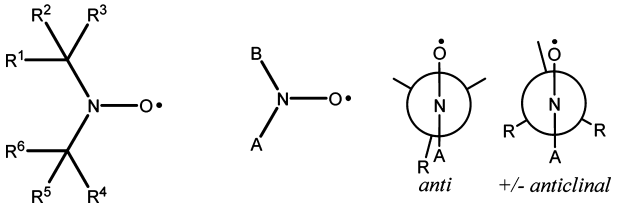

Figure 6. Description of polar/stabilization and steric effects in nitroxides.

For the C−ON bond homolysis, the bulkiness $E_{s,n}$ of fragments A and B is expressed by eq 21, where E_s(A or B) is the bulkiness for fragment A or B and ε is a term to describe the interaction between A and B. E_s(A or B) was estimated according to eq 22, developed by Fujita,[51] for which the values of individual steric constants $r(R_i)$ are ranked from the least bulky group $r(R_1)$ to the bulkiest group $r(R_3)$.[19,48,52] The k_c values for the C−ON bond re-formation of **1**$\alpha^\bullet$ and **6**$\alpha^\bullet$ with various alkyl radicals do not exhibit differences larger than a 1.5-fold factor, e.g., $k_{c,6\alpha^\bullet+a^\bullet}/k_{c,1\alpha^\bullet+a^\bullet} \approx 1.3$, $k_{c,6\alpha^\bullet+d^\bullet}/k_{c,1\alpha^\bullet+d^\bullet} \approx 1.5$,[29] $k_{c,1\alpha^\bullet+e^\bullet}/k_{c,6\alpha^\bullet+e^\bullet} \approx 1.1$,[25] $k_{c,6\alpha^\bullet+f^\bullet}/k_{c,1\alpha^\bullet+f^\bullet} \approx 1.1$,[25,26] and $k_{c,6\alpha^\bullet+g^\bullet}/k_{c,1\alpha^\bullet+g^\bullet} \approx 1.1$,[25] though the X-ray data and the conformations reported above show different conformations around the nitroxide moiety. This observation is in sharp contrast with the results reported for the C−ON bond homolysis, for which a striking difference of rate constant was observed for the same nitroxides.[53] It points out the absence of interaction between fragments A and B (ε = 0) and also that each group either in position anti to the N−O• or in the ±anticlinal position (dihedral angle ⟨RCNO$^\bullet$⟩ larger than 90°) to the N−O$^\bullet$ bond does not exert any steric effect, ($r(R_i)$ = 0). All individual $r(R_i)$ values are given in Table 2, and the $E_{s,n}$ values are given in Table 3.

$$E_{s,n} = E_s(\mathrm{A}) + E_s(\mathrm{B}) + \varepsilon \qquad (21)$$

$$E_s(\mathrm{A\ or\ B}) = -2.104 + 3.429[r(R_1)] + 1.978[r(R_2)] + 0.649[r(R_3)] \qquad (22)$$

Good correlations (high values for regression coefficients, Student *t* tests, and Student-Fischer *F* tests, Table 4) between the re-formation rate constants and the nitroxide properties (eqs 23 − 25, Table 4) were observed for alkyl radicals **a**• − **c**•, with only few deviating data. Due to larger series of k_c values and re-evaluated parameters,[23,24,32] coefficients δ' and ρ' given in Table 4 for **a**• and **b**• are different from those previously reported, but the signs are the same.[23,24]

The nitroxides carrying at least one phenyl group at the α position were not included in the correlations because the congestion due to a phenyl ring flanking the N−O$^\bullet$ moiety cannot be described accurately. Indeed, it has often been mentioned that the phenyl ring has to be considered as a *Janus*

Table 2. Individual Hammett Polar Constants σ_I and Individual Steric Constants $r(R_i)$

R[a]	σ_I[b]	$r(R_i)$[c]	R[a]	σ_I[b]	$r(R_i)$[c]	R[a]	σ_I[b]	$r(R_i)$[c]
H	0	0.32	$Me_2C{=}N-$	0.14[d]	*e*	MeCHOHCMeH−	0.01[f]	*e*
Me	−0.01	0	MeN=CMe−	0.35[d]	*e*	$MeCHOAcCH_2-$	0.04[f]	*e*
Et	−0.01	−0.38	PhMeC=N−	0.14[d]	*e*	MeCHOAcCMeH−	0.04[f]	*e*
i-Pr	+0.01	−1.08	MeN=CPh−	0.35[d]	*e*	$MeCHOBzCH_2-$	0.04[g]	*e*
n-Bu	−0.01	−0.70[h]	Me_2N-	0.17	*e*	$MeCHOHCH_2-$	0.03	*e*
t-Bu	−0.01	−2.46	$Me_2NCHMe-$	0.05[i]	*e*	$MeCOCH_2-$	0.11[f]	*e*
Ph	0.12	−1.40[j]	Me_2NCMe_2-	0.04[k]	*e*	MeCOCMeH−	0.09[f]	*e*
$-(CH_2)_5-$	−0.02[l]	−0.15[m]	$MeCHOHCH_2-$	0.03[f]	*e*	AcNBnCO	0.28[n]	*e*
$-(CH_2)_4-$	−0.02[l]	−0.04[m]	Me-*t*-BuNCO−	0.28[f]	*e*	$P(O)(OEt)_2$	0.32	−1.22[o]
CH_2OH	0.11	−0.06[f]	AcN-*t*-BuCH_2-	0.09[f]	*e*			

[a]Various groups for R^1−R^6. [b]Given in ref 49 unless otherwise mentioned. [c]Given in ref 51 unless otherwise mentioned. [d]It was assumed $\sigma_{I,Me2C=N} \approx \sigma_{I,PhMeC=N} \approx \sigma_{I,MeHC=N} \approx \sigma_{I,PhHC=N}$ = 0.14 and $\sigma_{I,PhC=NMe} \approx \sigma_{I,MeC=NMe} \approx \sigma_{I,HC=NPh}$ = 0.35 using $F_{PhHC=N}$ = 0.15 and $F_{HC=NPh}$ = 0.33 (and the subsequent equations) as given in ref 50. [e]Not estimated due to its *anti* position to the N−O• bond. [f]See ref 21. [g]Assuming $\sigma_{I,CH_2CMeHOC(O)Ph} = \sigma_{I,CH_2CHOAcMe}$ = 0.04. [h]Another value was applied; see text. [i]$\sigma_{I,NMe2}$ = 0.17 affording $\sigma_{I,CHMeNMe2}$ = 0.05; see refs 20 and 49. [j]The values applied depended on the nitroxide and the alkyl radical, see text. [k]$\sigma_{I,NMe2}$ = 0.17 affording $\sigma_{I,Me2NMe2C}$ = 0.04; see refs 20 and 49. [l]It was assumed the polar effect was the same as that of two methyl groups. [m]Other values were applied depending on the nitroxide, see text. [n]See ref 24. [o]Charton reported υ = 1.04 for $P(O)(OMe)_2$; see ref 57. When υ is converted into the E_s scale assuming isosteric equivalence with the *s*Bu group (υ = 1.02; see ref 54), it affords a E_s value of −1.38 for P(O)(OMe), very close to the value estimated in ref 19.

dx.doi.org/10.1021/jo300459z | J. Org. Chem. 2012, 77, 4996−5005

Table 3. Values of Stabilization/Polarity (σ_I) and Steric (E_s) Molecular Descriptors for Selected Nitroxides and Corresponding Coupling Rate Constants k_c with Alkyl Radicals a$^\bullet$−c$^\bullet$ [a]

			k_c (10^7 M^{-1} s^{-1})			
nitroxide	σ_I[b,c]	E_s[c,d]	a$^\bullet$ [e]	b$^\bullet$ [f]	c$^\bullet$ [f]	ref
1α$^\bullet$	−0.06	−4.20	23.7[g,h]	*i*	*i*	28
2α$^\bullet$	0.10	−7.25[j]/6.0[k]	0.80[h]	7.0[l]	*i*	29,[m,n] 30[m]
3α$^\bullet$	0.28	−8.22	0.30	0.5[l]	3.6[h,o,p,q]	29,[m,n] 34[r]
3β$^\bullet$	0.40	−8.26	0.30	*i*	*i*	29
5α$^\bullet$	0.45	−4.20	*i*	48.0	160.0[l]	32
5β$^\bullet$	0.45	−4.20	*i*	24.0[s]	120.0	32
5χ$^\bullet$	0.45	−6.21	*i*	*i*	46.0	32
5δ$^\bullet$	0.45	−6.21[t]	*i*	12.0	*i*	23
5ε$^\bullet$	0.18	−4.20	18.9[u]	140.4[l]	113.4[l]	t.w.,[m] 23[n,r]
5φ$^\bullet$	0.18	−5.21	13.9[u]	34.0	26.0	t.w.,[m] 23[n,r]
5γ$^\bullet$	0.18	−4.31	18.4[u]	86.0	70.0	t.w.[m] 23[n,r]
5η$^\bullet$	0.18	−5.21[t]	6.9[u]	34.0	38.0	23
5ι$^\bullet$	0.18	−5.21[v]	*i*	28.0	29.0	t.w.,[m] 23[n,r]
5φ$^\bullet$	0.18	−5.21	10.2[u]	34.0	*i*	23
5κ$^\bullet$	0.18	−6.21	3.5[u]	12.0	16.0	t.w.,[m] 23[n,r]
5λ$^\bullet$	0.18	−6.21[t]	2.1[u]	11.5[l]	*i*	t.w.,[m] 23[r]
5μ$^\bullet$	0.18	−4.2[w]	*i*	82.0	62.0	23
5ν$^\bullet$	0.18	−4.60[x]	13.0[u]	28.0	*i*	t.w.,[m] 23[n]
5ο$^\bullet$	0.44	−4.7[y]/−6.20[z]	11.2[u]	14.00	*i*	t.w.,[m] 23[n]
5π$^\bullet$	0.44	−5.7[y]/−7.20[z]	8.8[u]	5.70	*i*	t.w.,[m] 23[n]
5θ$^\bullet$ [aa]	0.08	−4.20	20.0[bb]	*i*	*i*	25
5ρ$^\bullet$ [aa]	0.08	−6.20	*i*	4.1[l]	*i*	29
5σ$^\bullet$	0.45	−5.21	*i*	17.0	*i*	t.w.
6α$^\bullet$ [aa]	−0.06	−4.20	18.3[h,bb,cc]	28.0[h,l,o,dd]	69.7	25,[m] 26,[m] 29,[m,n] 33[n,r]
6β$^\bullet$ [aa]	0.33	−4.20	26.00	*i*	*i*	27
6χ$^\bullet$ [aa]	0.33	−4.45	19.00	*i*	*i*	27
6δ$^\bullet$ [aa]	0.33	−4.70	12.00	*i*	*i*	27
6ε$^\bullet$ [aa]	0.33	−5.21	10.00	*i*	*i*	27
6φ$^\bullet$ [aa]	0.33	−5.21	10.00	*i*	*i*	27
6γ$^\bullet$ [aa]	0.33	−5.45	6.80	*i*	*i*	27
6η$^\bullet$ [aa]	0.33	−6.20	4.00	*i*	*i*	27
6ι$^\bullet$	0.02	−4.20	29.4[g]	*i*	*i*	28
6φ$^\bullet$	0.02	−5.21[aa]	5.80	*i*	*i*	24
6κ$^\bullet$	0.00	−4.70[aa]	6.10	*i*	*i*	24
6λ$^\bullet$	0.04	−4.70[aa]	8.10	*i*	*i*	24
6μ$^\bullet$	0.04	−4.20	28.5[g]	*i*	*i*	28
6ν$^\bullet$	0.16	−4.70[aa]	8.70	*i*	*i*	24
6ο$^\bullet$	0.52	−4.21[ee]	28.5[g]	*i*	*i*	28
9α$^\bullet$	−0.04	−2.94	57.3[bb]	*i*	*i*	25
10α$^\bullet$	0.79[ff]	−8.5[gg,hh]	0.7[o]	<1.3[o]	10.0[o]	31

[a]Structures are given in Figure 1. [b]Given by eq 20. [c]For individual values of $\sigma_{I,n}$ and $E_{s,n}$, see Table 2. [d]Given by eqs 21 and 22. [e]k_c given for *tert*-butylbenzene as solvent unless otherwise mentioned. [f]k_c given for benzene as solvent unless otherwise mentioned. [g]Correction for the acetonitrile solvent effect was given as k_c(*tert*-butylbenzene)/k_c(acetonitrile) = 3.0; see refs 25, 26, and 29. [h]Averaged value. [i]Not measured. [j]For the coupling with a$^\bullet$, r(Ph) = −1.40; see text. [k]For the coupling with b$^\bullet$, r(Ph) = −0.55; see text. [l]Correction for the acetonitrile solvent effect was given as k_c(benzene)/k_c(acetonitrile) = 1.8; see refs 25, 26, and 29. [m]For a$^\bullet$. [n]For b$^\bullet$. [o]Correction for the di-*tert*-butyl peroxide solvent effect was given as k_c(benzene)/k_c(di-*tert*-butyl peroxide) = 0.4; see refs 25, 26, 29, and 31. [p]Assuming weak penultimate unit effect for $Et_2NCHMeCH_2CHCOOMe$. [q]Correction for the triethylamine solvent effect was given as k_c(benzene)/k_c(triethylamine) = 0.5; see refs 25, 26, 29, and 31. [r]For c$^\bullet$. [s]k_c = 63.0 × 10^7 L s^{-1} mol^{-1} was previously reported in ref 23. [t]It was assumed that the cyclohexyl group was as sterically demanding as two ethyl groups. [u]Correction for the benzene solvent effect was given as k_c(*tert*-butylbenzene)/k_c(benzene) = 1.6; see refs 25, 26, and 29. [v]It was assumed that the two *n*-butyl groups were not sterically more demanding than the two ethyl groups. For other examples, see refs 19, 21, 23, and 24. [w]$E_{s,-(CH_2)_4-}$ = 0.00; see text. [x]$E_{s,-(CH_2)_4-}$ = 0.00, $E_{s,-(CH_2)_5-}$ = −0.15; see text. [y]For the coupling with a$^\bullet$, r(Ph) = −0.20; see text. [z]For the coupling with b$^\bullet$, r(Ph) = −0.76; see text. [aa]Given in ref 24. [bb]Correction for the isooctane solvent effect was given as k_c(isooctane)/k_c(*tert*-butylbenzene) = 1.5; see refs 25, 26, and 29. [cc]Assuming a weak penultimate unit effect of $Et_2NCHMeCH_2CHPh$ and discarding the values in 2,2,4-trimethylpentane[26] and acetonitrile,[28] and in di-*tert*-butyl peroxide.[31] [dd]Assuming a weak penultimate unit effect of $Et_2NCHMeCH_2CMeCOOMe$ in ref 31. Data in acetonitrile in ref 28 were discarded. [ee]$E_{s,-(CH_2)_5-}$ = 0.00; see text. [ff]It was assumed $\sigma_{I,2\text{-}(MeCNPh)C6H4}$ = $\sigma_{I,4\text{-}(MeCNPh)C6H4}$ = 0.20. $\sigma_{I,4\text{-}(MeCNPh)C6H4}$ was estimated as described in ref 47 using $\sigma_{I,MeN=CMe}$ and $\sigma^0_{R,Ac}$ = 0.20. [gg]r(Ph) = −1.63 for the coupling with a$^\bullet$−c$^\bullet$. [hh]The bulkiness of the aromatic ring conjugated to the nitroxyl moiety was assumed to be the same as for a methyl group syn to the N−O$^\bullet$.

dx.doi.org/10.1021/jo300459z | J. Org. Chem. 2012, 77, 4996−5005

Table 4. Correlation of log k_c at Room Temperature with a Linear Combination of the Molecular Descriptors (eq 19) Taking into Account the Steric Effect (E_s) and the Stabilization/Polar Effect (σ_I) of the Nitroxides for the Cross-Coupling Reaction with Alkyl Radicals a$^\bullet$ (Eq 23), b$^\bullet$ (Eq 24), and c$^\bullet$ (Eq 25)

eq	log $k_{c,0}$	δ'	ρ'_I	N^a	R^{2b}	s^c	t^d	F^e	E_s^f (%)	σ_I^f (%)
23	10.22(±0.10)	0.46(±0.02)	0.41(±0.17)	28	0.95	0.12	99.99^g	254	89	11
							97.70^h			
24	11.10(±0.25)	0.57(±0.05)	1.42(±0.18)	14	0.95	0.18	99.99^g	69	81	19
							98.00^h			
25	10.23(±0.16)	0.35(±0.03)	0.93(±0.25)	12	0.94	0.12	99.99^g	67	76	24
							99.50^h			

[a]Number of data. Outliers (empty symbols in Figure 7) and nitroxides carrying an aromatic group attached to the α position (stars in Figure 7) were not included. [b]Square of the linear regression coefficient. [c]Standard deviation. [d]Student t test given in percent. [e]Student−Fischer F test, at 99.99% level of confidence. [f]Equations given in ref 20. [g]For δ'. [h]For ρ'_I.

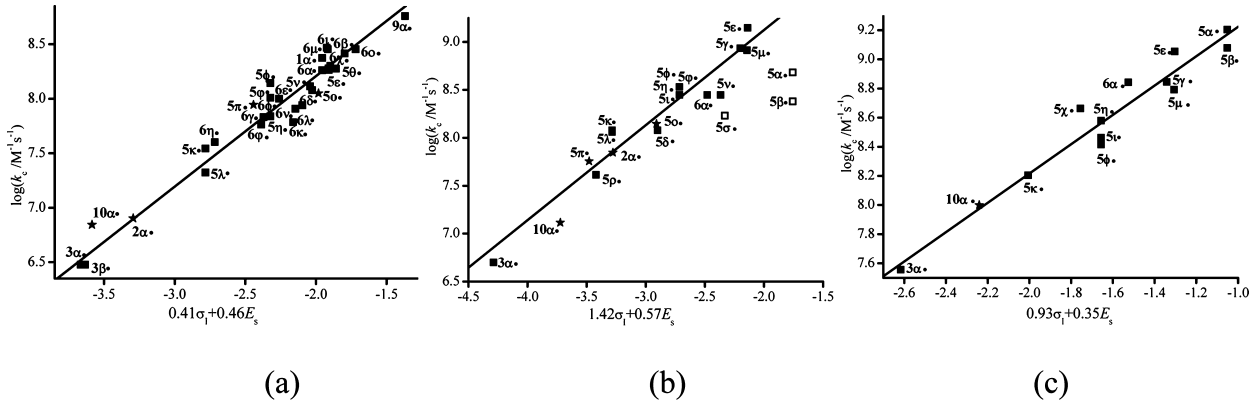

Figure 7. log k_c vs $f(\sigma_I, E_s)$ at room temperature for the cross-coupling of alkyl radicals (a) a$^\bullet$ in *tert*-butylbenzene (eq 23), (b) b$^\bullet$ in benzene (eq 24), and (c) c$^\bullet$ in benzene (eq 25) with various nitroxides (structures shown in Figure 1). Empty symbols denote outliers, and the asterisks denote nitroxides carrying an aromatic group attached to one carbon at the α position.

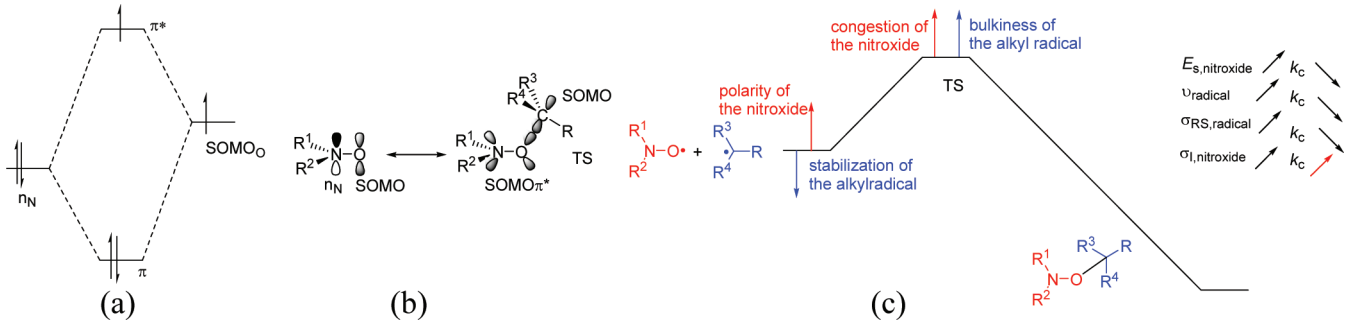

Figure 8. (a) Orbital diagram of the SOMO of the nitroxide. (b) Interaction between the SOMO π^* (nitroxide) and the SOMO (alkyl radical) at TS. (c) Effect of the polarity/stabilization of the nitroxide, the congestion around the nitroxyl moiety, the bulkiness, and the stabilization of the alkyl radical on the TS and initial state (starting materials).

group,[54−56] that is, its steric demand dramatically depends on its surroundings and on the reactant. This is nicely highlighted by the different values required for r(Ph) of **2α**$^\bullet$ (r = −1.40 for a$^\bullet$, r = −0.55 for b$^\bullet$), **5*o***$^\bullet$ and **5*π***$^\bullet$ (r = −0.20 for a$^\bullet$, r = −0.76 for b$^\bullet$), and **10α**$^\bullet$ (r = −1.63 for a$^\bullet$−c$^\bullet$) to fit eqs 23−25 describing the cross-coupling rate constants for a nitroxide with radicals a$^\bullet$, b$^\bullet$, and c$^\bullet$, respectively. The r(Ph) values applied for **5*o***$^\bullet$, **5*π***$^\bullet$, **10α**$^\bullet$, and **2α**$^\bullet$ (for b$^\bullet$) are different from the r(Ph) = −1.40 generally used for the correlation with k_d (Figure 7). Values of k_c for **5*ϕ***$^\bullet$ + b$^\bullet$, **5*η***$^\bullet$ + b$^\bullet$, **5*φ***$^\bullet$ + c$^\bullet$, **5*η***$^\bullet$ + c$^\bullet$, **5κ**$^\bullet$ + a$^\bullet$, **5λ**$^\bullet$ + a$^\bullet$, and **5κ**$^\bullet$ + b$^\bullet$, **5λ**$^\bullet$ + b$^\bullet$ show that the *spiro*-cyclohexyl ring moiety is as bulky as two ethyl groups. Thus, r(Et) values were used to describe the steric effect of the cyclohexyl group instead of $r(-(CH_2)_5-)$ = −0.15 for five-membered ring nitroxides.[19,21,51] However, for six-membered-ring nitroxides, a *spiro*-cyclohexyl group at the α position is not more sterically demanding than two methyl groups, i.e., $r(-(CH_2)_5-)$ = 0, as highlighted by **6*o***$^\bullet$ + a$^\bullet$. The deviation observed for the cross-coupling of b$^\bullet$ with **5α**$^\bullet$, **5β**$^\bullet$, and **5σ**$^\bullet$ cannot be straightforwardly taken into account.

As shown in Table 4, biparameter correlations yielded significantly improved statistical outputs. The weight of each effect on the rate constant k_c for each series of alkyl radical was estimated in the same way as had been done for k_d.[20] It comes out that the steric effect, i.e., the hampered approach of the nitroxyl moiety, is a more important effect (>75%) than the polar effect (<25%).

dx.doi.org/10.1021/jo300459z | J. Org. Chem. 2012, 77, 4996−5005

DISCUSSION

Correlations show that both the polar/stabilization and steric effects depend on the alkyl radical: that is, on their stabilization and their type (secondary for $\mathbf{a}^\bullet$ and $\mathbf{c}^\bullet$ and tertiary for $\mathbf{b}^\bullet$). Nevertheless, whatever the alkyl radical, the steric effect, which determines how significantly the approach of the alkyl radical is hampered by the congestion around the nitroxyl moiety, is the main effect (>75%). This effect is modified by the stabilization of the alkyl radical, i.e., $\delta'(\mathbf{c}^\bullet) < \delta'(\mathbf{a}^\bullet)$ as $\sigma_{RS,c}{}^\bullet < \sigma_{RS,a}{}^\bullet$ ($\sigma_{RS,a}{}^\bullet$ = 0.34 and $\sigma_{RS,c}{}^\bullet$ = 0.18).[20] All effects discussed below are related to the frontier molecular orbital interactions occurring at TS. The SOMO of the nitroxide is described as a three-electron bond orbital with the odd electron located in the π^* orbital (Figure 8a).[35] In such case, since the SOMO of the nitroxide is similar to a double bond, an approach of the alkyl radical through a Burgi−Dünitz trajectory is expected.[58] Consequently, this approach will depend dramatically on the congestion around the nitroxide moiety. As expected for a hampered approach, steric coefficients δ' are positive, and $\delta'(\mathbf{b}^\bullet)$ for tertiary alkyl radical is larger than $\delta'(\mathbf{a}^\bullet)$ and $\delta'(\mathbf{c}^\bullet)$ for secondary alkyl radicals. Furthermore, the efficiency of the cross-coupling reaction is related to the energy gap and to the overlapping between the SOMOs of the nitroxide (SOMO π^*, Figure 8b) and of the alkyl radical, as well as to the spin density in the SOMOs. These factors are hardly entangled and depend on both the steric and polar/stabilization effects. For example, radicals $\mathbf{b}^\bullet$ and $\mathbf{c}^\bullet$ exhibit very close radical stabilization ($\sigma_{RS,b}{}^\bullet$ = 0.20 and $\sigma_{RS,c}{}^\bullet$ = 0.18)[20] and polarity ($\sigma_{I,b}{}^\bullet$ = 0.07 and $\sigma_{I,c}{}^\bullet$ = 0.09).[20] Thus, $\delta'(\mathbf{b}^\bullet)$ being larger than $\delta'(\mathbf{c}^\bullet)$ means that the approach of $\mathbf{b}^\bullet$ is more hampered than that of $\mathbf{c}^\bullet$, since radical $\mathbf{b}^\bullet$ is bulkier than $\mathbf{c}^\bullet$ ($\upsilon_b{}^\bullet$ = 1.42 and $\upsilon_c{}^\bullet$ = 1.01),[20,59] and the orbital overlapping for $\mathbf{b}^\bullet$ is weaker than for $\mathbf{c}^\bullet$. On the other hand, radicals $\mathbf{a}^\bullet$ and $\mathbf{c}^\bullet$ exhibit very close bulkiness ($\upsilon_a{}^\bullet$ = 0.99 and $\upsilon_c{}^\bullet$ = 1.01)[20,59] and polarity ($\sigma_{I,a}{}^\bullet$ = 0.07 and $\sigma_{I,c}{}^\bullet$ = 0.09).[20] Consequently, $\delta'(\mathbf{a}^\bullet)$ being larger than $\delta'(\mathbf{c}^\bullet)$ points to a larger sensitivity of the cross-coupling reaction to the stabilization of the alkyl radical, since radical $\mathbf{a}^\bullet$ is more stabilized than $\mathbf{c}^\bullet$;[20] that is, the less stabilized the alkyl radical, the smaller the energy gap between the SOMOs and the less sensitive the reaction to the steric effect which hampers good orbital overlapping. The importance of the spin density (relocation of the odd electron onto the reactive radical center) of the SOMOs is nicely highlighted by $\rho'(\mathbf{b}^\bullet)$ being larger than $\rho'(\mathbf{c}^\bullet)$. In fact, the poor orbital overlapping for radical $\mathbf{b}^\bullet$ is partially balanced by a stronger polar effect due to the EWG group attached to the nitroxide moiety, which favors form **B** (high spin density on the oxygen atom) over form **A** and so the reaction with the poor overlapping is more sensitive to the polar effect, and the converse is true for radical $\mathbf{c}^\bullet$. Moreover, the less stabilized radical $\mathbf{c}^\bullet$ shows a higher polar effect ($\rho'(\mathbf{c}^\bullet) > \rho'(\mathbf{a}^\bullet)$) than radical $\mathbf{a}^\bullet$, because the odd electron is more relocalized on the reactive radical center and the orbital interaction is stronger with the "polar" nitroxides, for which form **B** is favored.[25,26]

According to the Hammond postulate, low activation energies E_a for the cross-coupling reactions imply that the TS is reactant-like. Hence, the congestion around the nitroxide moiety and the bulkiness of the alkyl radical destabilize the TS and cause the decrease in k_c. Stabilizing the alkyl radical stabilizes the reactant state and also causes the decrease in k_c. The increase in the polarity of the substituents on the nitroxide moiety destabilizes the reactant state, increasing k_c. The steric effect is better ascribed to an entropy effect and the stabilization/polarity effect to an enthalpy effect.

Application to NMP. A few years ago, Siegenthaler and Studer[60] investigated the NMP of styrene with alkoxyamines **6ρa**, **6πa**, and **6θa**. Although **6ρa** and **6πa** exhibit similar k_d values ($k_d = 6.7 \times 10^{-4}$ s^{-1} at 90 °C), a very different kinetic behavior was observed; i.e., the polymerization was much faster with $\mathbf{6\pi}^\bullet$ as controlling agent (6 h for 50% conversion, polydispersity index (PDI) is 1.15) than with $\mathbf{6\rho}^\bullet$ (29 h for 50% conversion, PDI = 1.15). Both reactions exhibited good control. On the other hand, for the polymerization controlled by $\mathbf{6\theta}^\bullet$ (for **6θa**, $k_d = 4.9 \times 10^{-3}$ s^{-1} at 90 °C), the polymerization time was even shorter (2 h for 67% conversion), but the control was poor (PDI = 1.76). *Such striking differences were attributed to the dramatic changes in $k_{c,ds}$ values.* Interestingly, when the Fischer diagram (Figure 9) was plotted for the NMP of styrene at 90 °C,[12,61] using k_d values reported in the literature[60] and k_c estimated values at room temperature,[62] it appeared that NMPs for $\mathbf{6\rho}^\bullet$ and $\mathbf{6\pi}^\bullet$ were expected to be highly controlled and living (living fraction LF larger than 80% and PDI ≈ 1.1) with a long time of polymerization ($t_{70\%}$ = 30 h). Although the polymerization times were shorter than those predicted, a shorter time had been observed with $\mathbf{6\pi}^\bullet$ than with $\mathbf{6\rho}^\bullet$, as expected. The shorter polymerization time is not surprising, since $k_{c,ds}$ and $k_{d,ds}$ can experience dramatic changes due to both the chain length effect and the temperature (k_c and $k_{c,ds}$ can decrease with increasing temperature) depending on the nitroxide.[12] In the Fischer diagram (Figure 9), $\mathbf{6\theta}^\bullet$ lies very close to the line of control; thus, it is not surprising that a poor control had been experimentally observed for this nitroxide. Unfortunately, the livingness had not been reported.

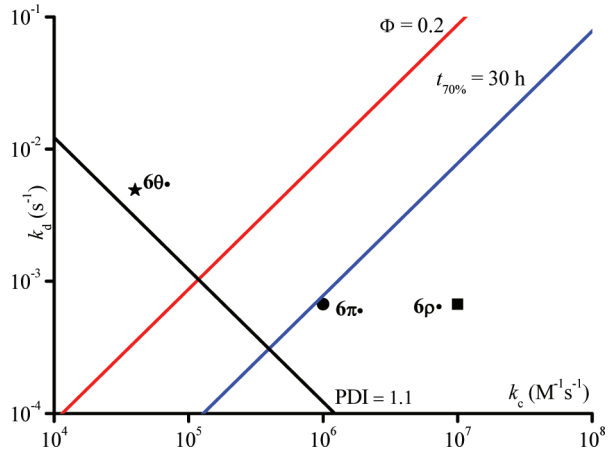

Figure 9. Fischer phase diagram for the NMP of styrene controlled by $\mathbf{6\pi}^\bullet$ (●), $\mathbf{6\theta}^\bullet$ (*) and $\mathbf{6\rho}^\bullet$ (■) at 90 °C: k_p = 900 M^{-1} s^{-1},[61] $k_t = 1.5 \times 10^8$ M^{-1} s^{-1},[61] concentration of initiating alkoxyamine **6ρa**, **6πa**, and **6θa** at 1 mol % for a targeted dead fraction Φ of 20%, a PDI of 1.1, and 70% conversion in 30 h.

CONCLUSION

The analysis of the coupling reactions of alkyl radicals $\mathbf{a}^\bullet$−$\mathbf{c}^\bullet$ with 39 nitroxides sheds a new light on the different effects involved in the cross-coupling reaction between nitroxides and alkyl radicals: (i) the stabilization of the alkyl radical, as well as the congestion at the nitroxide moiety, results in a decrease in k_c; (ii) the presence of EWG attached to the nitroxide moiety increases the odd electron density on the oxygen atom of the

dx.doi.org/10.1021/jo300459z | J. Org. Chem. 2012, 77, 4996−5005

nitroxide moiety and, hence, leads to the increase in k_c; (iii) the steric effect is mainly due to the groups flanking the nitroxide moiety, provided that the dihedral angles ⟨ONCR⟩ are smaller than 90°.[25,26] The recent studies of the effect of the protonation of the nitroxide on its cross-coupling reactions with **b**• and **c**• have shown a slight increase in k_c, as expected from eqs 21 and 22, since σ_I was increased by protonation.[50,63]

The example of the Fischer phase diagram applied to the NMP of styrene in the presence of **6***ρ*•, **6***π*•, and **6***θ*• nicely highlights the importance of k_c for the fate of NMP experiments. More detailed discussions and more examples of the importance of k_c for NMP will be provided in a forthcoming review.

EXPERIMENTAL SECTION

Nitroxides **5***β*•, **5***ε*•, **5***ϕ*•, **5***γ*•, **5***ι*•, **5***κ*•, **5***λ*•, **5***ν*•, **5***o*•, **5***π*•, and **5***σ*• were kindly provided by Dr. Kirilyuk. Distyryl ketone (DSK; Figure 1) and bis(*tert*-butoxycarbonyl-1-prop-1-yl) ketone (DPK) were prepared according to the literature.[64,65] Solvents were purchased and used as received. The rate constants k_c were measured by laser flash photolysis−kinetic absorption (LFP−KAS) with the setup and the experimental conditions described previously.[23]

AUTHOR INFORMATION

Corresponding Author

*E-mail: sylvain.marque@univ-provence.fr. Tel: +33(0)4-91-28-80-46. Fax: +33(0)4-91-28-87-58.

Notes

The authors declare no competing financial interest.

ACKNOWLEDGMENTS

We are grateful to Dr. I. Kirilyuk for providing the nitroxides and Dr. M. Edeleva and L. Tatarova for the help in DSK preparation. E.G.B. is grateful to the Division of Chemistry and Material Sciences (Grant 5.1.1) and the RFBR (Grant 12-04-01435) for funding. S.R.A.M. is grateful to the CNRS and RAS (Grants ASR 21244 and ASR23961) for funding the scientific exchange.

REFERENCES

(1) Solomon, D. H.; Rizzardo, E.; Cacioli, P. Eur. Pat. Appl. 135280, 1985; US Patent 4,581,429, 1986; *Chem. Abstr.* **1985**, *102*, 221335q.
(2) Hawker, C. J.; Bosman, A. W.; Harth, E. *Chem. Rev.* **2001**, *101*, 3661−3688.
(3) Braunecker, W. A; Matyjaszewski, K. *Prog. Polym. Sci.* **2007**, *32*, 93−146.
(4) Marque, S.; Gigmes, D. Nitroxide-Mediated Polymerization and its Applications. In *Encyclopedia of Radicals in Chemistry, Biology and Materials*; Chatgilialoglu, C., Studer, A., Eds.; Wiley: Chichester, U.K., 2012; pp 1813−1850.
(5) Fischer, H. *Chem. Rev.* **2001**, *101*, 3581−3610.
(6) Goto, A.; Fukuda, T. *Prog. Polym. Sci.* **2004**, *29*, 329−385.
(7) Moad, G.; Solomon, D. H. *The Chemistry of Radical Polymerization*, 2nd fully revised ed.; Elsevier: Amsterdam, 2006.
(8) *Handbook of Radical Polymerization*; Matyjazewski, K., Davis, T. P., Eds.; Wiley-Interscience: New York, 2002.
(9) Grubbs, R. B. *Polym. Rev.* **2011**, *51*, 104−137.
(10) Tebben, L.; Studer, A. *Angew. Chem. Int. Ed.* **2011**, *50*, 5034−5068.
(11) Bagryanskaya, E. G.; Marque, S. R. A. *Chem. Rev.* Manuscript in preparation
(12) Bertin, D.; Gigmes, D.; Marque, S. R. A.; Tordo, P. *Chem. Soc. Rev.* **2011**, *40*, 2189−2198.
(13) Bertin, D.; Gigmes, D.; Marque, S. R. A. *Recent Res. Dev. Org. Chem.* **2006**, *10*, 63−121 and references therein.
(14) Studer, A.; Schulte, T. *Chem. Rec.* **2005**, *5*, 27−35.
(15) Tebben, L.; Studer, A. *Angew. Chem., Int. Ed.* **2011**, *50*, 5034−5068.
(16) Greene, A. C.; Grubbs, R. B. *ACS Symp. Ser.* **2009**, *1024*, 81−93.
(17) Hodgson, J. L.; Lin, C.-Y.; Coote, M. L.; Marque, S. R. A.; Matyjaszewski, K. *Macromolecules* **2010**, *43* (8), 3728−3743.
(18) Lin, C. Y.; Marque, S. R. A.; Matyjaszewski, K.; Coote, M. L. *Macromolecules* **2011**, *44* (19), 7568−7583.
(19) Marque, S. *J. Org. Chem.* **2003**, *68* (20), 7582−7590.
(20) Bertin, D.; Gigmes, D.; Marque, S. R. A.; Tordo, P. *Macromolecules* **2005**, *38* (7), 2638−2650.
(21) Fischer, H.; Kramer, A.; Marque, S. R. A.; Nesvadba, P. *Macromolecules* **2005**, *38* (24), 9974−9984.
(22) Iwao, K.; Sakakibara, K.; Hirota, M. *J. Comput. Chem.* **1998**, *19*, 215−221.
(23) Zubenko, D.; Tsentalovich, Y.; Lebedeva, N.; Kirilyuk, I.; Roshchupkina, G.; Zhurko, I.; Reznikov, V.; Marque, S. R. A.; Bagryanskaya, E. *J. Org. Chem.* **2006**, *71* (16), 6044−6052.
(24) Fischer, H.; Marque, S. R. A.; Nesvadba, P. *Helv. Chim. Acta* **2006**, *89*, 2330−2340.
(25) Bowry, V. W.; Ingold, K. U. *J. Am. Chem. Soc.* **1992**, *114*, 4992.
(26) Beckwith, A. L. J.; Bowry, V. W.; Ingold, K. U. *J. Am. Chem. Soc.* **1992**, *114*, 4983−4992.
(27) Marque, S.; Sobek, J.; Fischer, H.; Kramer, A.; Nesvadba, P.; Wunderlich, W. *Macromolecules* **2003**, *36*, 3440−3442.
(28) Skene, W. G.; Scaiano, J. C.; Listigover, N. A.; Kazmaier, P. M.; Georges, M. K. *Macromolecules* **2000**, *33*, 5065.
(29) Sobek, J.; Martschke, R.; Fischer, H. *J. Am. Chem. Soc.* **2001**, *123*, 2849−2857.
(30) Le Mercier, C.; Lutz, J.-F.; Marque, S.; Le Moigne, F.; Tordo, P.; Lacroix-Desmazes, P.; Boutevin, B.; Couturier, J.-L.; Guerret, O.; Martschke, R.; Sobek, J.; Fischer, H. *ACS Symp. Ser.* **2000**, *768*, 108−122.
(31) Lalevee, J.; Gigmes, D.; Bertin, D.; AllonaS, X.; Fouassier, J.-P. *Chem. Phys. Lett.* **2007**, *449*, 231−235.
(32) Zubenko, D; Kirilyuk, I.; Roschchupkina, G.; Zhurko, I.; Reznikov, V.; Marque, S. R. A.; Bagryanskaya, E. *Helv. Chim. Acta* **2006**, *89*, 2341−2353.
(33) Lebedeva, N.; Zubenko, D. P.; Bagryanskaya, E. G.; Sagdeev, R. Z.; Ananchenko, G. S.; Marque, S.; Bertin, D.; Tordo, P. *Phys. Chem. Chem. Phys.* **2004**, *6*, 2254−2259.
(34) Ananchenko, G. S.; Souaille, M.; Fischer, H.; Le Mercier, C.; Tordo, P. *J. Polym. Sci.: Polym. Chem.* **2002**, *40*, 3264−3283.
(35) Karoui, H.; Le Moigne, F.; Ouari, O.; Tordo, P. In *Stable Radicals: Fundamentals and Applied Aspects of Odd-Electron Compounds*; Hicks, R., Ed.; Wiley: Hoboken, NJ, 2010; pp 173−229 and references therein.
(36) Family **4**• is reserved for the nitroxide carrying an $EtSOCH_2$ group attached to the *α* carbon of the nitroxide. Families **7**• and **8**• are ascribed to seven- and eight-membered-ring nitroxides. These three families are not investigated in this article.
(37) Calculations showed that six-membered-ring nitroxides prefer, in general, to adopt a twist-boat conformation close to the twist conformation of five-membered-ring nitroxides: Billone, P. S.; Johnson, P. A.; Lin, S.; DiLabio, G.; Ingold, K. U. *J. Org. Chem.* **2011**, *76*, 631−636.
(38) Debuigne, A.; Chang-Sen, D.; Li, L. I.; Hamer, G. K.; Georges, M. K. *Macromolecules* **2007**, *40*, 6224−6232.
(39) Studer, A.; Harms, K.; Knoop, C.; Muller, C.; Schulte, T. *Macromolecules* **2004**, *37*, 27−34.
(40) Marque, S.; Fischer, H.; Baier, E.; Studer, A. *J. Org. Chem.* **2001**, *66*, 1146−1156.
(41) Acerbis, S.; Bertin, D.; Boutevin, B.; Gigmes, D.; Lacroix-Desmazes, P.; Le Mercier, C.; Lutz, J.-F.; Marque, S. R. A.; Siri, D.; Tordo, P. *Helv. Chim. Acta* **2006**, *89* (10), 2119−2132.
(42) The intramolecular H bonding of **3***β*• deracemized the two enantiomers, keeping the geometrical parameters very close to each other.[41]

(43) The diethylphosphoryl group of **3α•** was replaced by the dibenzylphosphoryl group in **3χ•**: Grimaldi, S.; Siri, D.; Finet, J.-P.; Tordo, P. *Acta Crystallogr., Sect. C: Cryst. Struct. Commun.* **1998**, *54*, 1712.
(44) It can be argued that the different conformations reported for the **2•** and **3•** families might be due to the π−π interaction occurring between the π systems of the amide and aromatic groups of **2β•** strengthened by the crystal effect (π stacking). Therefore, it may occur that in solution the preferred conformation would be closer to that reported for **3α•**. Nevertheless, this has no importance for the estimated $E_{s,2\alpha^\bullet}$, $E_{s,3\alpha^\bullet}$, and $E_{s,3\beta^\bullet}$ values.
(45) Mendenhall, G. D.; Ingold, K. U. *J. Am. Chem. Soc* **1973**, *95*, 6395−6400.
(46) Ananchenko, G.; Beaudoin, E.; Bertin, D.; Gigmes, D.; Lagarde, P.; Marque, S. R. A.; Revalor, E.; Tordo, P. *J. Phys. Org. Chem.* **2006**, *19* (4), 269−275.
(47) Bertin, D.; Gigmes, D.; Marque, S. R. A.; Milardo, S.; Peri, J.; Tordo, P. *Collect. Czech. Chem. Commun.* **2004**, *69* (12), 2223−2238.
(48) Beaudoin, E.; Bertin, D.; Gigmes, D.; Marque, S. R. A.; Siri, D.; Tordo, P. *Eur. J. Org. Chem.* **2006**, *7*, 1755−1768.
(49) Charton, M. *Prog. Phys. Org. Chem.* **1981**, *13*, 119−251.
(50) Hansch, C.; Leo, A.; Taft, R. W. *Chem. Rev.* **1991**, *91*, 165−195.
(51) Fujita, T.; Takayama, C.; Nakajima, M. *J. Org. Chem.* **1973**, *38*, 1623−1630.
(52) Bagryanskaya, E.; Bertin, D.; Gigmes, D.; Kirilyuk, I.; Marque, S. R. A.; Reznikov, V.; Roshchupkina, G.; Zhurko, I.; Zubenko, D. *Macromol. Chem. Phys.* **2008**, *209*, 1345−1357.
(53) It was shown that the size and the position of the substitution/hybridization, and also the type of nitroxide, i.e., cyclic such as **6α•** or noncyclic such as **1α•**, strongly influenced k_d; e.g., the homolysis of **1α**a was 20 times faster than for **6α**a.[19,21]
(54) Unger, S. H.; Hansch, C. *Prog. Phys. Org. Chem.* **1976**, *12*, 91−118.
(55) Kutter, E.; Hansch, C. *J. Med. Chem.* **1969**, *12*, 647−652.
(56) The phenyl group is considered as a *Janus* group; that is, it can adopt many conformations involving several possible values for *r*(Ph).[54,55] For the C—ON bond homolysis of **5o**b, it was shown that *r*(Ph) = −0.23 was a suitable value for geminate phenyl groups.[52]
(57) Charton, M. *Top. Curr. Chem.* **1983**, *114*, 57−91.
(58) Braslau, R.; Naik, N.; Zipse, H. *J. Am. Chem. Soc.* **2000**, *122*, 8421−8434.
(59) For alkyl radical, the Charton steric parameter υ was preferred.[20,57]
(60) Siegenthaler, K. O.; Studer, A. *Macromolecules* **2006**, *39*, 1347−1352.
(61) For k_p and k_t, see: Beuermann, S.; Buback, M. *Prog. Polym. Sci.* **2002**, *27*, 191−254.
(62) k_c values were estimated using eq 20, and $E_{s,Et}$ = −0.38, $E_{s,Me3SiOCHMe}$ = −2.46, $E_{s,Me3SiOCHiPr}$ = −4.47, $E_{s,CH2OSiMe2tBu}$ = −0.65, and σ_I = −0.06. Unfortunately, the E_s values were only rough estimates and were expected to be larger.
(63) Values of k_c were not estimated because reliable values of σ_I for the nitroxide could not be developed upon protonation.
(64) Baretz, B. H.; Turro, N. J. *J. Am. Chem. Soc.* **1983**, *105*, 1309.
(65) Knühl, B.; Marque, S; Fischer, H. *Helv. Chim. Acta* **2001**, *84*, 2290.